

Functionalized pyrazine-2-carboxamides in the synthesis of new palladium-based potential cytotoxic agents

Svetlana G. Churusova,^a Aleksandr V. Konovalov,^a Diana V. Aleksanyan,^{*a}
Ekaterina Yu. Rybalkina,^b Yulia V. Nelyubina,^c Svetlana A. Soloveva,^d Aleksandr S. Peregudov,^a
Zinaida S. Klemenkova^a and Vladimir A. Kozlov^a

^a A. N. Nesmeyanov Institute of Organoelement Compounds, Russian Academy of Sciences,
119334 Moscow, Russian Federation. E-mail: aleksanyan.diana@ineos.ac.ru

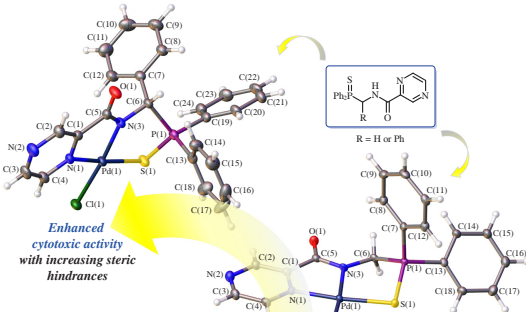
^b N. N. Blokhin National Medical Research Center of Oncology, 115478 Moscow,
Russian Federation

^c Federal Research Center of Problems of Chemical Physics and Medicinal Chemistry,
Russian Academy of Sciences, 142432 Chernogolovka, Moscow Region, Russian Federation

^d N. D. Zelinsky Institute of Organic Chemistry, Russian Academy of Sciences, 119991 Moscow,
Russian Federation

DOI: 10.71267/mencom.7819

The reactions of α -(aminoalkyl)diphenylphosphine sulfides with pyrazine-2-carbonyl chloride hydrochloride afforded two novel representatives of non-classical amide-based pincer ligands. The latter were shown to furnish Pd^{II} complexes with either bi- or tridentate coordination modes of the ligands, depending on the reaction conditions. The cytotoxicity assays revealed remarkable activity of one of the resulting cyclopalladated derivatives, especially, towards hematopoietic cancer cell lines.



Keywords: carboxamides, pyrazines, phosphine sulfides, pincer ligands, palladium, cyclometalation, metal-based anticancer agents.

High stability and tunability of pincer complexes, provided by a specific tridentate monoanionic ligand framework, laid a firm basis for their continuous research in organic synthesis and catalysis.^{1–4} However, a recent decade has witnessed a growing interest in their biological and medicinal applications, including the discovery of pincer-type entities in active sites of some enzymes⁵ and the development of potential antitumor agents.⁶ In this context, of particular interest are the pincer systems based on functionalized carboxamides which can be readily obtained by a simple modular assembly of building blocks and smoothly undergo direct cyclometalation, affording a robust metal–nitrogen bond with the central amide unit (see, for example, complexes A–G in Figure 1).^{7–15}

Recently, we have shown that (aminoalkyl)diphenylphosphine sulfides could serve as useful synthons in the design of picolinamide ligands for cytotoxic Pd^{II} complexes.⁷ This and earlier studies^{7–9} of our research group revealed that a combination of the soft and hard ancillary donor centers could be the key to enhanced bioactivity of such complexes. Therefore, it seemed interesting to combine a thiophosphoryl group with another N-heterocyclic unit in a non-classical amide-based pincer backbone to further explore the anticancer properties of ensuing Pd^{II} complexes. In this communication, we present the synthesis of thiophosphoryl-functionalized pyrazine-2-carboxamides and their complexing features towards Pd^{II} ions, as well as the results of cytotoxicity screening of the complexes obtained.

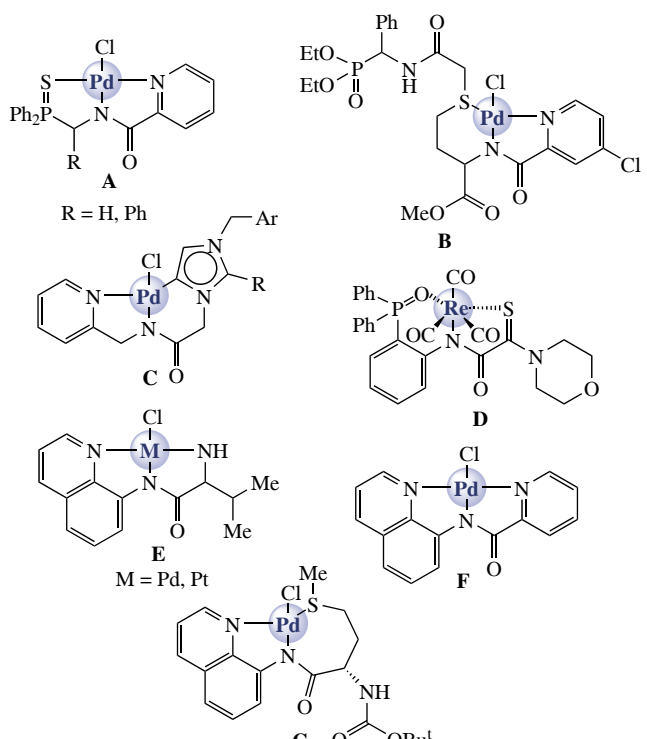
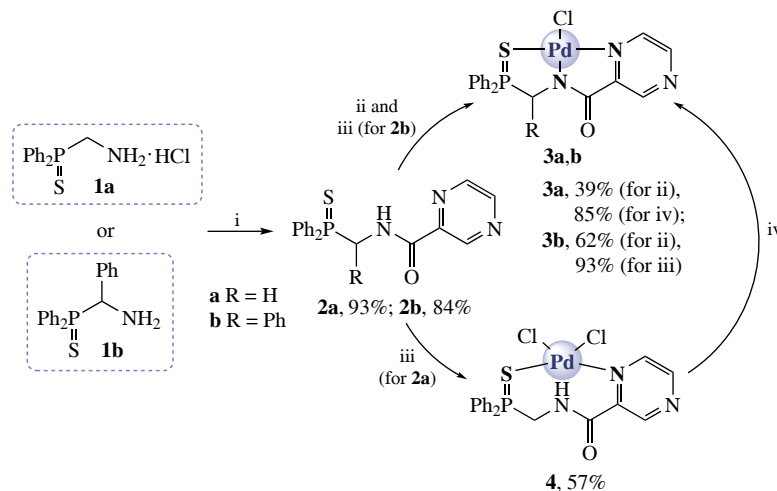


Figure 1 Biologically active carboxamide-based transition metal pincer complexes.



Scheme 1 Reagents and conditions: i, Et_3N , pyrazine-2-carbonyl chloride hydrochloride, CH_2Cl_2 , $-5 \rightarrow 0$ °C, 30 min, then room temperature, 1 day; ii, $(\text{PhCN})_2\text{PdCl}_2$, Et_3N , CH_2Cl_2 , room temperature, 1 day; iii, $(\text{PhCN})_2\text{PdCl}_2$, MeCN , room temperature, 1 day; iv, DMSO , room temperature, 2 days (^1H NMR monitoring).

The condensation of α -(aminomethyl)- and α -(aminobenzyl)-diphenylphosphine sulfides **1a,b**⁷ with pyrazine-2-carbonyl chloride hydrochloride smoothly afforded carboxamides **2a,b** in high yields (Scheme 1).

To study the peculiarities of the direct cyclopalladation of compounds **2a,b**, we probed their reactivity towards Pd^{II} ions both in the presence and in the absence of a base. The reaction of amide **2a** with a versatile cyclopalladating agent, $(\text{PhCN})_2\text{PdCl}_2$, under the standard conditions, *i.e.*, in dichloromethane upon addition of Et_3N afforded the target pincer-type complex only in 39% yield. The analogous reaction of its phenyl-substituted counterpart **2b** provided a significantly better result: the yield of complex **3b** reached 61%, equating to the values observed for the related picolinamide-based derivatives.⁷ This is not surprising since additional steric factors can force pincer-type coordination. However, even in this case the crude reaction product contained free pyrazine-2-carboxamide **2b**. The latter is likely to result from the partial reduction of the cyclopalladated product under the action of Et_3N , rather than the low reactivity. Note that Et_3N is usually used to facilitate the formation of a pincer-type complex through binding HCl , liberated upon metalation, but can also have an adverse effect on N-metallated species.¹⁶ Indeed, the reaction of **2b** with the same metal precursor in MeCN at room temperature without addition of a base smoothly afforded Pd^{II} pincer complex **3b** in an excellent yield. At the same time, treatment of thiophosphorylmethyl-appended derivative **2a** with $(\text{PhCN})_2\text{PdCl}_2$ in MeCN in the absence of a base yielded mainly bidentately bound complex **4** which precipitated from the reaction mixture. The low solubility of compound **4** seems to be the main obstacle for its further transformation into the pincer-type product. Thus, in DMSO it gradually converts to complex **3a**, affording about 85% of the pincer derivative in 2 days after dissolution (see Online Supplementary Materials, Figure S27).

The realization of a tridentate monoanionic pincer-type coordination of the deprotonated pyrazine-2-carboxamides in complexes **3a,b** was unequivocally confirmed by the IR and NMR spectroscopic data (including the results of different 2D NMR experiments). Thus, a strong downfield shift of the phosphorus resonance indicated binding of the thiophosphoryl group by the metal ions [$\Delta\delta_{\text{P}} = 20.7$ ppm (**3a**) and 16.3 ppm (**3b**)], which was also reflected in a significant displacement of the ^{13}C NMR signals corresponding to the methylene and methine bridges in the amine component ($\Delta\delta_{\text{C}} = 11.8$ –13.3 ppm). The signals for the CH unit adjacent to one of the pyrazine nitrogen atoms (C^4 carbon nucleus and the connected proton, for

the numbering scheme see Online Supplementary Materials) were found to be considerably deshielded upon complexation, with $\Delta\delta_{\text{C}}$ and $\Delta\delta_{\text{H}}$ values exceeding 5.0 and 0.25 ppm, respectively. Finally, the deprotonation was evidenced by the lack of the NH proton signal in the ^1H NMR spectra as well as the absence of the corresponding absorption bands of the free secondary amide group in the IR spectra of the resulting palladacycles (for example, $\nu_{\text{N}-\text{H}}$). In turn, a neutral bidentate coordination mode of ligand **2a** in complex **4** with the intact $\text{C}(\text{O})\text{NH}$ unit was deduced from the presence of an amide II band at 1517 cm^{-1} , associated with $\text{N}-\text{H}$ bending and $\text{C}-\text{N}$ stretching vibrations, as well as a strongly shifted $\text{P}=\text{S}$ absorption band at 581 cm^{-1} . Moreover, the ^1H NMR spectrum recorded after its dissolution in DMSO revealed a broadened downfield singlet of the NH proton, the characteristic virtual triplet for the methylene protons, as well as the deshielded signal for the $(\text{C}^4)\text{H}$ proton of the pyrazine ring. In all cases, the identities of the resulting complexes were confirmed by the elemental analyses.

The structures of palladacycles **3a,b** were further confirmed by single-crystal X-ray diffraction (Figure 2).[†] In both cases, the

[†] Crystal data for **3a**. $\text{C}_{18}\text{H}_{15}\text{ClN}_3\text{OPPdS}$ ($M = 494.21$), monoclinic, space group $P2_1$, $a = 9.18800(4)$, $b = 17.40690(9)$ and $c = 11.45413(6)$ \AA , $\alpha = \gamma = 90^\circ$, $\beta = 92.4845(4)^\circ$, $V = 1830.190(15)$ \AA^3 , $Z = 4$, $T = 100$ K, $\mu(\text{Mo-K}\alpha) = 115.27$ cm^{-1} , $d_{\text{calc}} = 1.794$ g cm^{-1} . Total of 47723 reflections were measured, and 7987 independent reflections ($R_{\text{int}} = 0.0338$) were used in the further refinement. The refinement converged to $wR_2 = 0.0639$ and $\text{GOF} = 1.086$ for all independent reflections [$R_1 = 0.0232$ was calculated against F for 7976 observed reflections with $I > 2\sigma(I)$].

Crystal data for **3b**. $\text{C}_{24.75}\text{H}_{19.75}\text{C}_{13.25}\text{N}_3\text{OPPdS}$ ($M = 659.83$), triclinic, space group $P\bar{1}$, $a = 11.4067(3)$, $b = 12.7995(3)$ and $c = 19.9818(5)$ \AA , $\alpha = 75.7520(10)$, $\beta = 75.2950(10)$, and $\gamma = 74.6960(10)^\circ$, $V = 2671.09(12)$ \AA^3 , $Z = 4$, $T = 120$ K, $\mu(\text{Mo-K}\alpha) = 11.82$ cm^{-1} , $d_{\text{calc}} = 1.641$ g cm^{-1} . Total of 32802 reflections were measured, and 14129 independent reflections ($R_{\text{int}} = 0.0322$) were used in the further refinement. The refinement converged to $wR_2 = 0.0784$ and $\text{GOF} = 0.997$ for all independent reflections [$R_1 = 0.0330$ was calculated against F for 10385 observed reflections with $I > 2\sigma(I)$].

Single crystals were obtained by slow diffusion of Et_2O into CH_2Cl_2 solutions of compounds **3a,b**. The data for **3b** were collected with a Bruker APEXII CCD diffractometer, using graphite monochromated $\text{Mo-K}\alpha$ radiation ($\lambda = 0.71073$ \AA). The data for **3a** were collected on a four-circle Rigaku Synergy S diffractometer equipped with a HyPix6000HE area-detector (kappa geometry, shutterless ω -scan technique, graphite monochromated $\text{Cu-K}\alpha$ -radiation). The intensity data were integrated and corrected for absorption and decay by the CrysAlisPro program (version 1.171.41.106a, Rigaku Oxford Diffraction, 2021). All the structures were solved with the SHELXT¹⁷ structure

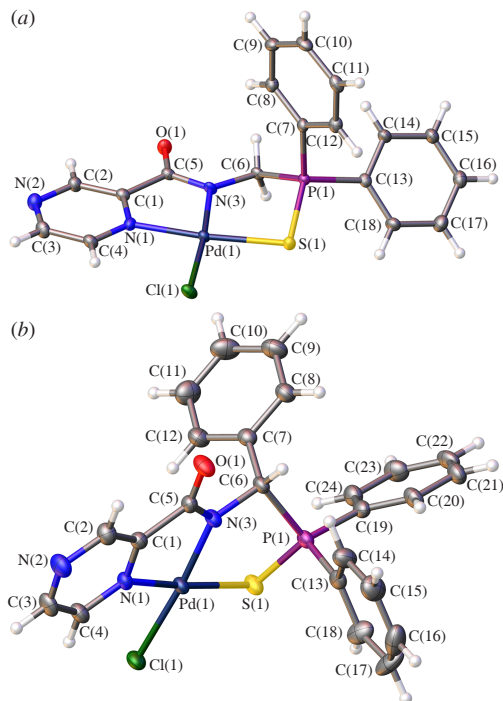


Figure 2 General view of (a) complex **3a** and (b) complex **3b** in representation of non-hydrogen atoms as thermal ellipsoids at $p = 45\%$. The second symmetry independent molecules are omitted for clarity.

Pd atom adopted a slightly distorted square-planar geometry, binding with the sulfur atom of the thiophosphoryl group, chloride anion, and nitrogen atoms of the pyrazine and deprotonated amide units.

The preliminary evaluation of the anticancer potential of the resulting compounds revealed that thiophosphorylmethyl-appended pincer complex **3a** was almost inactive against several human cancer cell lines, leading to more than 60 and 50% of living solid and hematopoietic cancer cells, respectively, at a concentration as high as $60\text{ }\mu\text{M}$ (Table 1). Its bidentately bound precursor **4** exerted only low cytotoxic effects against colon (HCT116), prostate (PC3), chronic myelogenous leukemia (K562 and doxorubicin-resistant subline K562/iS9), and multiple plasmacytoma (AMO1) cells, with the IC_{50} values ranging within $32\text{--}40\text{ }\mu\text{M}$. However, the instability of this derivative in DMSO raises serious concerns about the nature of the active species. At the same time, phenyl-substituted pincer complex **3b** exhibited moderate cytotoxicity towards the tested solid cancer cells and quite a high efficiency against blood cancer cell lineages, with the IC_{50} values down to $3.8\text{ }\mu\text{M}$. Although this complex was somewhat inferior to its picolinamide-based prototype,⁷ especially against solid cancer cell lines, it outperformed compound **A** (when $\text{R} = \text{Ph}$, see Figure 1) in terms of the toxicity towards conditionally normal human embryonic kidney cells HEK293 (consider the values of IC_{50} : 22.0 vs. $6.2\text{ }\mu\text{M}$, respectively). Furthermore, the selectivity towards the

solution program using Intrinsic Phasing and refined with the **XL¹⁸** refinement package using Least Squares minimization against F_{hkl}^2 in anisotropic approximation for non-hydrogen atoms in the Olex2 program.¹⁹ The positions of hydrogen atoms were calculated, and they were refined in the isotropic approximation within the riding model. Severely disordered molecules of chloroform in **3b** were treated as diffuse contributions to the overall scattering without specific atom positions using the Solvent Mask routine as implemented in Olex2.

CCDC 2448827 and 2448828 contain the supplementary crystallographic information for this paper. These data can be obtained free of charge from The Cambridge Crystallographic Data Centre via <https://www.ccdc.cam.ac.uk>.

Table 1 Cytotoxicity of the Pd^{II} pincer complexes based on pyrazine-2-carboxamides against selected human cell lines.

Cell line	$\text{IC}_{50} \pm \text{SD}, \text{ }\mu\text{M}$		
	3a	3b	Cisplatin
<i>Solid cancer cell lines</i>			
HCT116	>60.0	17.7 ± 0.5	18.0 ± 2.0
MCF7	>60.0	22.0 ± 2.0	25.0 ± 4.0
PC3	>60.0	15.5 ± 1.5	16.0 ± 3.0
<i>Hematopoietic cancer cell lines</i>			
K562	>60.0	4.8 ± 0.2	15.5 ± 0.5
K562/iS9	>60.0	7.1 ± 1.1	16.0 ± 2.0
AMO1	>60.0	3.8 ± 0.2	3.2 ± 0.6
MOLT4	>60.0	5.6 ± 0.6	6.5 ± 1.0
<i>Non-cancerous cell lines</i>			
HEK293	>60.0	22.0 ± 2.2	12.5 ± 1.5
HBL100	>60.0	19.0 ± 3.4	14.6 ± 3.6
HBL100/dox	>60.0	24.0 ± 2.5	23.6 ± 3.6

^aSD is the standard deviation of the value.

hematopoietic cancer cell lines over HEK293 lineage distinguishes palladocycle **3b** from the reference cisplatin. Note that the free pyrazine-2-carboxamides were non-toxic against all the cell lines explored even at a concentration of $60\text{ }\mu\text{M}$, which unambiguously indicates that the anticancer properties of their Pd^{II} complexes are stipulated by the presence of coordinated metal ions. Taking into account the low affinity of related amide-based pincer complexes to DNA,⁹ this type of cyclopalladated derivatives deserves further study.

Hence, even a minor structural modification of the thiophosphoryl-functionalized carboxamide backbone, such as a variation in an acid component, can lead to significant alterations in the cytotoxic properties of their cyclopalladated derivatives, from the substantial reduction in the effectiveness to significant enhancement of the selectivity.

This paper is dedicated to the centenary of the birth of Tatyana A. Mastryukova, the corresponding member of the Russian Academy of Sciences and the former head of the Group of Organothiophosphorus Compounds of INEOS RAS.

This work was supported by The Russian Science Foundation (grant no. 22-73-10044). The NMR studies and XRD analysis of complex **3b** were performed using the equipment of the Center for Collective Use of INEOS RAS with financial support from the Ministry of Science and Higher Education of the Russian Federation (agreement no. 075-00276-25-00). The crystal structure determination for compound **3a** was performed in the Department of Structural Studies of Zelinsky Institute of Organic Chemistry, Moscow. The cell growth inhibition studies were performed with financial support from the Ministry of Health of the Russian Federation (project no. 123021500068-8 NUYO-2023-0009, 2023–2025).

Online Supplementary Materials

Supplementary data associated with this article can be found in the online version at doi: 10.71267/mencom.7819.

References

1. K. K. Manar and P. Ren, *Adv. Organomet. Chem.*, 2021, **76**, 185; <https://doi.org/10.1016/bs.adomc.2021.04.003>.
2. L. Piccirilli, D. L. J. Pinheiro and M. Nielsen, *Catalysts*, 2020, **10**, 773; <https://doi.org/10.3390/catal10070773>.
3. J.-K. Liu, J.-F. Gong and M.-P. Song, *Org. Biomol. Chem.*, 2019, **17**, 6069; <https://doi.org/10.1039/c9ob00401g>.
4. H. Valdés, M. A. García-Eleno, D. Canseco-Gonzalez and D. Morales-Morales, *ChemCatChem*, 2018, **10**, 3136; <https://doi.org/10.1002/cctc.201702019>.

5 J. L. Nevarez, A. Turmo, J. Hu and R. P. Hausinger, *ChemCatChem*, 2020, **12**, 4242; <https://doi.org/10.1002/cctc.202000575>.

6 S. Wu, Z. Wu, Q. Ge, X. Zheng and Z. Yang, *Org. Biomol. Chem.*, 2021, **19**, 5254; <https://doi.org/10.1039/D1OB00577D>.

7 A. V. Konovalov, S. G. Churusova, D. V. Aleksanyan, E. Yu. Rybalkina, S. A. Aksanova, A. S. Peregudov, Z. S. Klemenkova and V. A. Kozlov, *Org. Biomol. Chem.*, 2023, **21**, 8379; <https://doi.org/10.1039/D3OB01309J>.

8 H. H. Nguyen, Q. T. Pham, Q. M. Phung, C. D. Le, T. T. Pham, T. N. O. Pham and C. T. Pham, *J. Mol. Struct.*, 2022, **1269**, 133871; <https://doi.org/10.1016/j.molstruc.2022.133871>.

9 S. G. Churusova, D. V. Aleksanyan, E. Yu. Rybalkina, E. I. Gutsul, A. S. Peregudov, Z. S. Klemenkova, Yu. V. Nelyubina, A. G. Buyanovskaya and V. A. Kozlov, *J. Inorg. Biochem.*, 2022, **235**, 111908; <https://doi.org/10.1016/j.jinorgbio.2022.111908>.

10 R. O. Omondi, N. R. S. Sibuyi, A. O. Fadaka, M. Meyer, D. Jaganyi and S. O. Ojwach, *Dalton Trans.*, 2021, **50**, 8127; <https://doi.org/10.1039/d1dt00412c>.

11 D. V. Aleksanyan, S. G. Churusova, E. Yu. Rybalkina, Yu. V. Nelyubina and V. A. Kozlov, *INEOS OPEN*, 2021, **4**, 237; <https://doi.org/10.32931/io2128a>.

12 M. Kiani, M. Bagherzadeh, S. Meghdadi, F. Fadaei-Tirani, K. Schenk-Joß and N. Rabiee, *Appl. Organomet. Chem.*, 2020, **34**, e5531; <https://doi.org/10.1002/aoc.5531>.

13 D. V. Aleksanyan, S. G. Churusova, V. V. Brunova, E. Yu. Rybalkina, O. Yu. Susova, A. S. Peregudov, Z. S. Klemenkova, G. L. Denisov and V. A. Kozlov, *J. Organomet. Chem.*, 2020, **926**, 121498; <https://doi.org/10.1016/j.jorgchem.2020.121498>.

14 J.-Y. Lee, J.-Y. Lee, Y.-Y. Chang, C.-H. Hu, N. M. Wang and H. M. Lee, *Organometallics*, 2015, **34**, 4359; <https://doi.org/10.1021/acs.organomet.5b00586>.

15 L. Yan, X. Wang, Y. Wang, Y. Zhang, Y. Li and Z. Guo, *J. Inorg. Biochem.*, 2012, **106**, 46; <https://doi.org/10.1016/j.jinorgbio.2011.09.032>.

16 V. Yu. Alekseenko, E. V. Sharova, O. I. Artyushin, D. V. Aleksanyan, Z. S. Klemenkova, Yu. V. Nelyubina, P. V. Petrovskii, V. A. Kozlov and I. L. Odinets, *Polyhedron*, 2013, **51**, 168; <https://doi.org/10.1016/j.poly.2012.12.025>.

17 G. M. Sheldrick, *Acta Crystallogr., Sect. A: Found. Adv.*, 2015, **71**, 3; <https://doi.org/10.1107/S2053273314026370>.

18 G. M. Sheldrick, *Acta Crystallogr., Sect. A: Found. Adv.*, 2008, **64**, 112; <https://doi.org/10.1107/S0108767307043930>.

19 O. V. Dolomanov, L. J. Bourhis, R. J. Gildea, J. A. K. Howard and H. Puschmann, *J. Appl. Crystallogr.*, 2009, **42**, 339; <https://doi.org/10.1107/S0021889808042726>.

Received: 7th May 2025; Com. 25/7819